Cardosin B PSI Transiently Expressed in Arabidopsis Lines with Alterations of ER Structure Is Secreted to the Extracellular Space in Cotyledon Cells [†]

Tatiana Cardoso [1], Susana Pereira [1,2], José Pissarra [1,2] and Cláudia Pereira [1,2,*]

[1] Faculdade de Ciências da Universidade do Porto, Rua do Campo Alegre, s/nº, 4169-007 Porto, Portugal; up201505769@up.pt (T.C.); mspereir@fc.up.pt (S.P.); jpissarr@fc.up.pt (J.P.)

[2] GreenUPorto—Sustainable Agrifood Production Research Center, Rua do Campo Alegre s/n, 4169-007 Porto, Portugal

[*] Correspondence: cpereira@&fc.up.pt

[†] Presented at the 2nd International Electronic Conference on Plant Sciences—10th Anniversary of Journal Plants, 1–15 December 2021; Available online: https://iecps2021.sciforum.net/.

Abstract: The ER is considered the hub of the secretory pathway, as newly synthesized proteins are distributed to other organelles from this location. The goal of this study was to understand ER impact in vacuolar sorting by combining *Arabidopsis thaliana* mutants with altered ER structure with the expression of known vacuolar markers. The mutants nai GFP-h and leb-2 GFP-h were selected from the NASC database and were transiently transformed with PSI-B fused with mCherry. Confocal Microscopy analysis showed that PSI-B is secreted in nai GFP-h and, to a lesser extent, in leb-2 GFP-h, which was confirmed in a secretion assay. Given that PSI-B mediates trafficking to the vacuole, it is intriguing to find it extracellularly in these mutant lines and we discussed whether the alterations in the ER may have a role in this process.

Keywords: Plant Specific Insert; protein trafficking; protein sorting; endoplasmic reticulum; *Arabidopsis thaliana*; electron microscopy; confocal microscopy

1. Introduction

The endomembrane trafficking system of eukaryotic cells is vital for important cellular functions, upholding cellular homeostasis and proliferation, as well as specific requirements characteristic of multicellular organisms [1,2]. The secretory pathway of plant cells has its gateway in the ER, an adaptable and versatile organelle that forms a three-dimensional network of continuous tubules and cisterns contacting with several organelles in the cell, such as the PM, the Golgi, endosomes, lysosomes, mitochondria, and peroxisomes, and coordinating with multiple membrane compartments along both the secretory and endocytic pathways [3–5]. In plants, unlike what we see in yeast and animal cells, the ER is confined to a small space of cytoplasm between the PM and the vacuolar membrane, while being extensively distributed and showing considerable movement in the cell [6,7]. Some organisms may even develop characteristic ER-derived structures, as the ER bodies, that are cylindrical compartments for the accumulation of large amounts of b-glucosidase (PYK10), which may be involved in plant defence, and are found in Brassicaceae plants and some related species [8,9].

The conventional trafficking through the secretory pathway takes proteins from the ER and leads them through the Golgi apparatus until their final destination, which might be the vacuole, other compartments, or the plasma membrane [10,11]. As plant cells have two different types of vacuoles (PSVs and LVs) and both may co-exist within the same cell [12,13], it is important to understand the mechanisms and regulation behind vacuolar trafficking, as vacuoles play a central role in plant cell homeostasis. Our laboratory has been

using as working models cardosin A and cardosin B, which are well-characterized APs found in *Cynara cardunculus* [14,15]. Despite being highly similar regarding protein sequence, these enzymes accumulate in different cell compartments during plant development [15,16]. Cardosin A has been shown to accumulate in PSVs or LVs, depending on the development stage and specific cellular needs [16–19], whereas cardosin B is found extracellularly [15]. However, when expressed in *Arabidopsis thaliana* and *Nicotiana tabacum*, both cardosins A and B were detected in LVs [20–22]. Such characteristics make cardosins intriguing and provide solid evidence for their utility as reporters for the study of vacuolar trafficking and VSDs in plants.

Plant Specific Inserts (PSIs) consist of unique protein domains of about 100 amino acids [23,24], frequently described "an enzyme within an enzyme", since, when isolated and in vitro, it presents several functions such as: acting as a detergent, mediating lipid membrane interactions, presents putative antimicrobial activity and can to induce membrane permeabilization, along with membrane modulation [25–29]. Although its functions in cells still need to be clarified, some reports have associated the PSI domain with vacuolar targeting of the APs [21,26,30]. As novel unconventional routes for vacuolar sorting, where proteins are directly sorted to the LV from the ER [21,31–34], are being revealed, it is necessary to understand where the PSI fits in the complex network of vacuolar protein trafficking. Even if both the cardosin A PSI (PSI A) and the cardosin B PSI (PSI B) can lead the AP to the vacuole, how each PSI does it is very different. The transport from the ER to the Golgi in PSI B-mediated sorting is COPII-dependent, whereas PSI A-mediated sorting is COPII-independent [35]. Moreover, and despite PSIs being considered to be vacuolar sorting determinants given their abilities to mediate trafficking to the vacuole, little is known regarding the mechanisms controlling this sorting. To understand in more detail the mechanisms of PSIs-mediated sorting, and since the ER seems to be a crucial checkpoint in these routes, we hypothesized if defects at the ER level lead to changes in protein sorting. As so, using the Nottingham Arabidopsis Stock Centre (NASC) database, we searched and selected *Arabidopsis thaliana* lines with mutations in genes leading to alterations in ER morphology and analysed the expression and localization of the PSI domain.

2. Material and Methods

2.1. Biological Material—Selection, Germination, and Growth Conditions

Resorting to the Nottingham Arabidopsis Stock Centre (NASC), two *Arabidopsis thaliana* lines described as having defects in ER morphology or mutations in ER-resident proteins were selected: N69075 (*nai GFP-h*) [36] and N69081 (*leb-2 GFP-h*—unpublished). These lines also harbour a GFP-HDEL marker that allows ER visualization. Seeds from those lines, as well as a wild type (WT; *col0*), were sown and germinated in plates containing MS (Mourashige and Skooge, Duchefa) medium with 1.5% (w/v) sucrose. Plants were kept for 48 h at 4 °C and, after stratification, were grown at 22 °C with 60% humidity and 16h light over 8h dark photoperiod (OSRAM L 36W/77 e OSRAM L 36W/840) at the intensity of 110 µmol m^{-2} s. After 12-15 days, seedlings were transferred to individual pots with fertilized substrate (SYRO PLANT) and grown under continuous light at 22 °C with 50–60% relative humidity and light intensity at 180 µmol m^{-2} s.

2.2. Vacuum Infiltration for Transient Transformation of Arabidopsis thaliana Seedlings

For transient transformation of *A. thaliana* the protocol established by Bernat-Silvestre et al. [37] was adapted. Seeds from *A. thaliana* mutated lines and wild type were sown and germinated in six-well plates and grown for 5 days under the conditions already described. For the transformation, *A. tumefaciens* harbouring SP-PSIB-mCherry construct [35] was inoculated in LB medium with the appropriate antibiotics [Kanamycin (50 µg/mL) and Gentamicin (50 µg/mL)] and incubated for 24 h in agitation at 28 °C, till an OD600 of 2.2. The culture was centrifuged for 15 min at 6000× *g* at room temperature and the pellet resuspended in infiltration buffer (liquid MS medium with 0.005% (v/v) Tween

and 200 μM acetosyringone). This suspension was kept at room temperature for 30-45 min and the suspension was poured onto the six-well plates with the *A. thaliana* seedlings (4 mL per well) and vacuum was applied at 300 mbar for 1 min. The pressure was then slowly increased to 400 mbar and vacuum applied for another minute. Finally, the bacterial suspension was removed, and the plates were covered with aluminium foil for 45 min to 1 h to improve agroinfection. The aluminium foil was then removed, and the plates were kept for 3 days under the previously mentioned growth conditions.

2.3. Drug Treatment Assays

Brefeldin A (BFA) solution (50 μg/mL) was prepared in MS liquid medium and 4 mL per well were poured over the infiltrated seedlings one day after the *A. tumefaciens* infiltration. Vacuum was applied as previously described (Section 2.2). Seedlings were kept in the BFA solution for about 16–18 h before the cells were imaged.

2.4. CLSM Analysis

A. thaliana seedlings were observed and analysed using a Confocal Laser Scanning Microscope (CLSM, Leica STELLARIS 8). Cotyledons from *A. thaliana* seedlings were prepared by placing the biological material on a slide with a drop of sterile water covered by a cover slip. In all situations the lower epidermis was observed. For mCherry, using 561 nm excitation, the emission was detected between 580–630 nm. In the case of GFP, the excitation used was 488 nm and the emission was detected between 500–528 nm. Analysis and quantification of the acquired images were performed using the ImageJ®/Fiji software.

2.5. Extraction of Extracellular Proteins

Agro-infiltrated and BFA-infiltrated seedlings were cut into thin strips and incubated in 1x extraction buffer (0.1 M NaCl, 4 mM HEPES pH 7.0, 0.5 mM DTT and 0.2 mM EDTA) under agitation (120 rpm) for 6 h at room temperature in the dark. It was used 1 mL of buffer per 100 mg of seeding tissue. After incubation, the buffer was collected, filtered with a 100 μM nylon mesh and centrifuged at 13,000× *g* for 10–15 min at 4 °C. The supernatant was collected and kept at −20 °C. To the defrosted extracellular samples, 1 mL of 20% (w/v) Tri-chloroacetic acid (TCA) was added per mL of medium and the tubes vortexed for 15 sec. These were kept on ice for 15 min before centrifugation at 13,000× *g* for 15 min at 4 °C. The supernatant was discarded, 1 mL of ice-cold acetone was added to the pellet, and the tubes were centrifuged as before. This wash was repeated, and the pellet left to air-dry. The pellet was resuspended 40 μL of extraction buffer and the samples were quantified in a DS-11 Spectophotometer (DeNovix). SDS-PAGE sample loading dye (Nzytech) was added, and samples were boiled at 95 °C for 5 min before being centrifuged for 2 min at top speed.

2.6. Western Blot Analysis

For the analysis of extracellular proteins samples, a 12% SDS-PAGE coupled to Western blotting was performed, as described previously [35]. The same protein amount of each sample was applied to the gel along with the protein weight marker PageRuler Plus Prestained Protein Ladder (Thermo Fisher). For the blot, the primary antibodies—Anti-mCherry (Merk Millipore) and H3 Histone 3 core (Agrisera)—were diluted (1:1000 and 1:5000, respectively) in blocking solution [5% (w/v) skim milk and 0.5% (v/v) Tween-20 in TBS-T] and incubation was performed at 4 °C overnight with agitation. The incubation with the secondary antibodies—Goat Anti-Rabbit IgG (H+L) HRP Conjugate and Goat Anti-Mouse IgG (H+L) HRP Conjugate (BioRad) -, diluted in TBS-T (1:2500 and 1:500, respectively), occurred at room temperature for 1 h in agitation. The visualization of the bands was carried out using the Clarity ECL Western Blotting Substrate Kit (BioRad), following the manufacture's instruction, and the imaging was acquired with ChemiDoc XRS+ System (BioRad) and the analysis was performed using the ImageJ® software.

3. Results

The heterologous expression of the PSI-B in Arabidopsis allowed to assess the localization of this domain in the cell. Several images of each condition were captured and analysed and the most representative are presented. Moreover, a quantitative approach of the PSI-B localization is also shown giving a more complete perception of the patterns observed.

3.1. *Expression and Localisation of PSI-B in ER-Defective Plants*

Regarding PSI B localization some differences can be observed between WT and mutant lines. In the WT line, PSI B was mostly observed accumulating in the vacuole and in some cells it was also secreted to the extracellular space (Figure 1A). In nai GFP-h, PSI B was found to be mostly secreted, although some accumulation in the vacuole was still observed (Figure 1B) and in leb-2 GFP-h it is mainly accumulating in the vacuole (Figure 1C). Quantification of the distribution patterns observed for these lines shows a clear tendency for more secretion in the nai GFP-h line, when compared to control, while in the leb-2 GFP-h less secretion can be observed (Figure 2A).
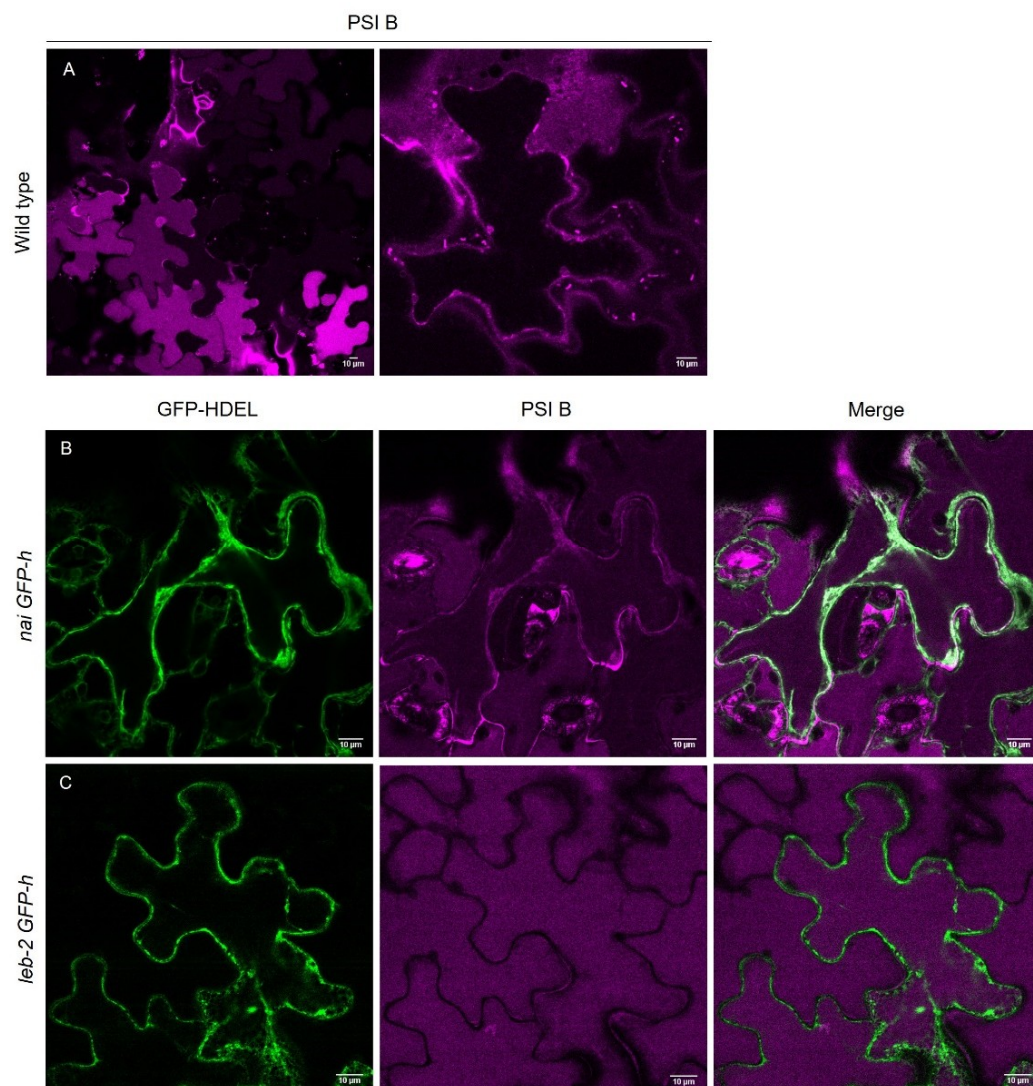

Figure 1. Subcellular localization of PSI B-mCherry in cotyledons of Arabidopsis thaliana wild type and ER-defective seedlings. (**A**) Expression of PSI B-mCherry in wild type; (**B**,**C**) Expression of PSI B-mCherry in nai GFP-h and in leb-2 GFP-h, respectively, which possess a GFP marked for ER retention. All observations and images were acquired 3 days post-infiltration. Scale bars: 10 μm.

Next, we assessed if these patterns of accumulation were affected by Brefeldin A (BFA). BFA is a fungal macrocyclic lactone widely used as an inhibitor of secretion and vacuolar protein transport in plant cells, causing the formation of ER-Golgi hybrid compartments [38]. Upon addition of the drug, the secretion observed in the untreated condition was decreased, but some accumulation in the extracellular space was still visible (not shown). Except for the leb-2 GFP-h, where PSI B was only found to accumulate in the vacuole, the other lines analysed presented the PSI B in the vacuole and secreted. In the WT this secretion was much less pronounced after BFA treatment as in the nai GFP-h lines, as it can be appreciated in the quantification (Figure 2B).
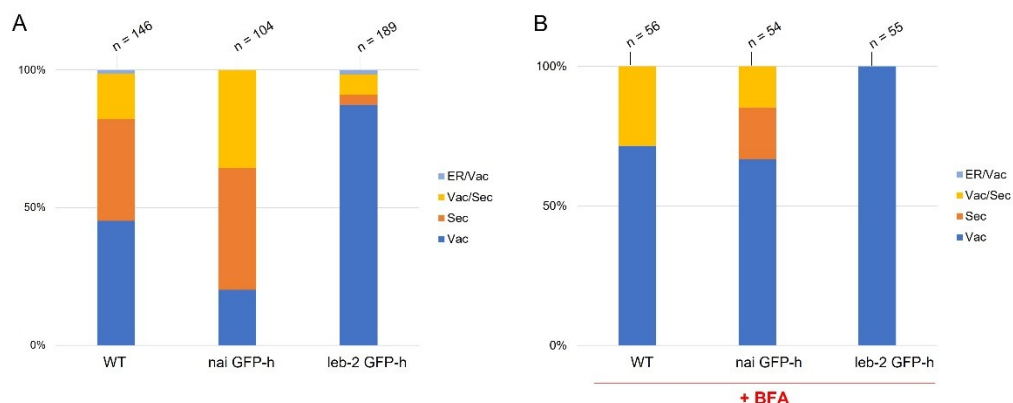

Figure 2. Quantification of PSI-B in cotyledons of Arabidopsis thaliana wild type and ER-defective seedlings in control conditions (**A**) and upon BFA treatment (**B**). The n above the bars refers to the number of cells counted. The PSIs were considered "secreted" when found at the cell periphery (cell wall) and/or extracellularly. Abbreviations: ER, endoplasmic reticulum; Sec, secreted; Vac, vacuole.

3.2. Secretion Assays

Given the extended secretion observed in some lines expressing PSI B, we decided to further confirm this event by isolating the extracellular protein content of seedlings from the WT and mutated lines infiltrated with PSI B fused with mCherry, with and without BFA. In this assay, a double control system was used: the control sample was an extract of the total protein content of seedlings that stably express the PSI B (unpublished data) and, to ensure that the bands obtained were not from intracellular proteins, an antibody against the H3 histone, a protein exclusively found in the intracellular content, was also used in the same protein extracts. Indeed, as observed through Confocal Microscopy, the PSI B-mCherry, with an expected size of 37 kDa, was detected in the extracellular protein content of the nai GFP-h and leb-2 GPF-h lines infiltrated with this domain (Figure 3).

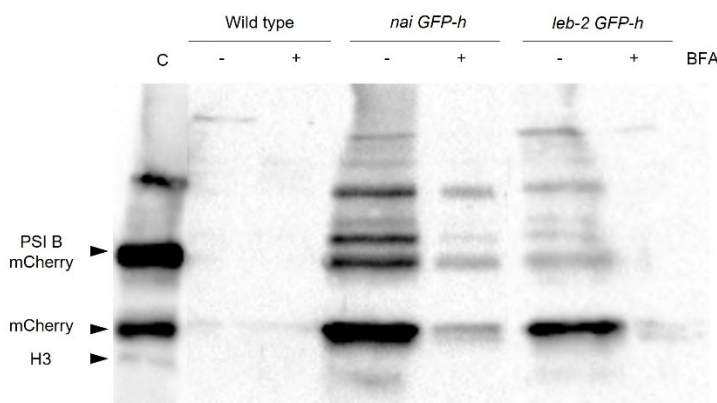**Figure 3.** Detection of PSIB-mCherry in extracelular protein extrats from Arabidopsis thaliana wild type and mutated lines. Western blot uisng a specific antibody against mCherry and Histone H3 (as

a burst control). The arrows indicate the bands corresponding to the PSI B-mCherry, the isolated mCherry and the histone H3. The minus sign indicates the absence of BFA treatment, and the plus sign indicates the presence of BFA treatment. Abbreviations: C, control sample.

Moreover, the decrease in secretion observed in CLSM imaging upon BFA treatment was also confirmed by the Western blot (Figure 3, lines "−" and "+" BFA). However, regarding the WT line, the PSI B was only faintly detected in the blot for both situations analyzed (with and without BFA treatment). The histone H3 has an expected size of 17 kDa, and is not detected in the extracellular proteins' samples.

4. Discussion

For the past years, cardosins and their PSI domains have been the focus of several studies, given the contributions of these domains to unveil unconventional vacuolar sorting routes [35,39]. In fact, the PSI B domain can direct proteins to the vacuole but does not match any classical VSD type. Moreover, the route mediated by the PSI B is COPII-dependent and follows the conventional ER-Golgi-Vacuole pathway [35]. In *Cynara cardunculus*, cardosin B is accumulated in the extracellular matrix of both stigma and style transmitting tissue [15], while in heterologous systems (Arabidopsis and Tobacco) it is accumulated in the LVs [22]. Such features highlight the advantage of this domain as reporter for the study of vacuolar trafficking and VSDs in plants.

We started this study by assessing if the ER defects exhibited by the mutated lines had any influence in the localization and trafficking of PSI B. Results obtained revealed that in the WT line the major site for this domain's accumulation was the vacuolar compartment, although some PSI B was also secreted to the extracellular space. Interestingly, the two mutated lines observed show variations of this phenotype: in the leb-2 GFP-h mutant PSI B is mainly accumulating in the vacuole while in nai GFP-h it was found to be mostly secreted. Despite more information is needed to fully understand how alterations in the ultrastructure influences how the proteins leave ER, the shift towards the vacuole or cell wall are an indication that indeed the ER integrity is crucial for signal recognition. The work of Soares da Costa and coworkers [22] described cardosin B's accumulation in the LVs, but the authors also mention its detection at the cell wall. Given its location in the native system (*Cynara cardunculus*), cardosin B's secretion has been suggested to be tissue specific [17], with cardosin B being secreted in specialized organs, such as flowers and seeds and vacuolar in vegetative tissues, which are the case of fully expanded leaves. It is worth noting, that the images presented here correspond to the cotyledonary cells and we may argue that these cells constitute a transition stage with characteristics and cellular machinery of both seed tissue and vegetative tissue. Nevertheless, it seems an interesting stage to uncover in more detail the mechanisms of PSI B, and as consequence cardosin B mediated sorting. As a whole, this work provides new insights on PSI B-mediated protein trafficking and how it is influenced by the structure and physiology of the organelles, such as defects in ER morphology or mutations in ER-resident proteins.

References

1. Morita, M.T.; Shimada, T. The Plant Endomembrane System—A Complex Network Supporting Plant Development and Physiology. *Plant Cell Physiol.* **2014**, *55*, 667–671. https://doi.org/10.1093/pcp/pcu049.
2. Cevher-Keskin, B. Endomembrane Trafficking in Plants. *Electrodialysis* **2020**, 1–22. https://doi.org/10.5772/intechopen.91642.
3. Staehelin, L.A. The plant ER: A dynamic organelle composed of a large number of discrete functional domains. *Plant J.* **1997**, *11*, 1151–1165. https://doi.org/10.1046/j.1365-313X.1997.11061151.x.
4. Stefan, C.J.; Manford, A.G.; Emr, S.D. ER-PM connections: Sites of information transfer and inter-organelle communication. *Curr. Opin. Cell Biol.* **2013**, *25*, 434–442. https://doi.org/10.1016/j.ceb.2013.02.020.
5. Stefano, G.; Renna, L.; Lai, Y.; Slabaugh, E.; Mannino, N.; Buono, R.A.; Otegui, M.S.; Brandizzi, F. ER network homeostasis is critical for plant endosome streaming and endocytosis. *Cell Discov.* **2015**, *1*, 15033. https://doi.org/10.1038/celldisc.2015.33.
6. Nakano, R.T.; Matsushima, R.; Ueda, H.; Tamura, K.; Shimada, T.; Li, L.; Hayashi, Y.; Kondo, M.; Nishimura, M.; Hara-Nishimura, I. GNOM-LIKE1/ERMO1 and SEC24a/ERMO2 Are Required for Maintenance of Endoplasmic Reticulum Morphology in Arabidopsis thaliana. *Plant Cell* **2009**, *21*, 3672–3685. https://doi.org/10.1105/tpc.109.068270.
7. Quader, H.; Schnepf, E. Endoplasmic reticulum and cytoplasmic streaming: Fluorescence microscopical observations in adaxial epidermis cells of onion bulb scales. *Protoplasma* **1986**, *131*, 250–252. https://doi.org/10.1007/BF01282989.
8. Matsushima, R.; Hayashi, Y.; Yamada, K.; Shimada, T.; Nishimura, M.; Hara-Nishimura, I. The ER Body, a Novel Endoplasmic Reticulum-Derived Structure in Arabidopsis. *Plant Cell Physiol.* **2003**, *44*, 661–666. https://doi.org/10.1093/pcp/pcg089.
9. Hara-Nishimura, I.; Matsushima, R.; Shimada, T.; Nishimura, M. Diversity and Formation of Endoplasmic Reticulum-Derived Compartments in Plants. Are These Compartments Specific to Plant Cells? *Plant Physiol.* **2004**, *136*, 3435–3439. https://doi.org/10.1104/pp.104.053876.
10. Marcos Lousa, C.; Gershlick, D.C.; Denecke, J. Mechanisms and Concepts Paving the Way towards a Complete Transport Cycle of Plant Vacuolar Sorting Receptors. *Plant Cell* **2012**, *24*, 1714–1732. https://doi.org/10.1105/tpc.112.095679.
11. Rojo, E.; Denecke, J. What is moving in the secretory pathway of plants? *Plant Physiol.* **2008**, *147*, 1493–503. https://doi.org/10.1104/pp.108.124552.
12. Olbrich, A.; Hillmer, S.; Hinz, G.; Oliviusson, P.; Robinson, D.G. Newly formed vacuoles in root meristems of barley and pea seedlings have characteristics of both protein storage and lytic vacuoles. *Plant Physiol.* **2007**, *145*, 1383–1394. https://doi.org/10.1104/pp.107.108985.
13. Paris, N.; Stanley, C.M.; Jones, R.L.; Rogers, J.C. Plant Cells Contain Two Functionally Distinct Vacuolar Compartments. *Cell* **1996**, *85*, 563–572. https://doi.org/10.1016/S0092-8674(00)81256-8.
14. Ramalho-Santos, M.; Verissimo, P.; Cortes, L.; Samyn, B.; Van Beeumen, J.; Pires, E.; Faro, C. Identification and proteolytic processing of procardosin A. *Eur. J. Biochem.* **1998**, *255*, 133–138. https://doi.org/10.1046/j.1432-1327.1998.2550133.x.
15. Vieira, M.; Pissarra, J.; Veríssimo, P.; Castanheira, P.; Costa, Y.; Pires, E.; Faro, C. Molecular cloning and characterization of cDNA encoding cardosin B, an aspartic proteinase accumulating extracellularly in the transmitting tissue of Cynara cardunculus L. *Plant Mol. Biol.* **2001**, *45*, 529–39.
16. Ramalho-Santos, M.; Pissarra, J.; Veríssimo, P.; Pereira, S.; Salema, R.; Pires, E.; Faro, C.J. Cardosin A, an abundant aspartic proteinase, accumulates in protein storage vacuoles in the stigmatic papillae of Cynara cardunculus L. *Planta* **1997**, *203*. https://doi.org/10.1007/s004250050183.
17. Pissarra, J.; Pereira, C.; Soares, D.; Figueiredo, R.; Duarte, P.; Teixeira, J.; Pereira, S.; Costa, D.S. da; Figueiredo, R.; Duarte, P.; et al. From Flower to Seed Germination in Cynara cardunculus: A Role for Aspartic Proteinases. *Int. J. Plant Dev. Biol.* **2007**, *1*, 274–281.
18. Pereira, C.S.; da Costa, D.S.; Pereira, S.; de Moura Nogueira, F.; Albuquerque, P.M.; Teixeira, J.; Faro, C.; Pissarra, J. Cardosins in postembryonic development of cardoon: Towards an elucidation of the biological function of plant aspartic proteinases. *Protoplasma* **2008**, *232*, 203–213. https://doi.org/10.1007/s00709-008-0288-9.
19. Oliveira, A.; Pereira, C.; Costa, D.S. d. D.S. da; Teixeira, J.; Fidalgo, F.; Pereira, S.; Pissarra, J. Characterization of aspartic proteinases in C. cardunculus L. callus tissue for its prospective transformation. *Plant Sci.* **2010**, *178*, 140–146. https://doi.org/10.1016/j.plantsci.2009.11.008.
20. Duarte, P.; Pissarra, J.; Moore, I. Processing and trafficking of a single isoform of the aspartic proteinase cardosin A on the vacuolar pathway. *Planta* **2008**, *227*, 1255–1268. https://doi.org/10.1007/s00425-008-0697-1.
21. Pereira, C.; Pereira, S.; Satiat-Jeunemaitre, B.; Pissarra, J. Cardosin A contains two vacuolar sorting signals using different vacuolar routes in tobacco epidermal cells. *Plant J.* **2013**, *76*, 87–100. https://doi.org/10.1111/tpj.12274.
22. da Costa, D.S.; Pereira, S.; Moore, I.; Pissarra, J. Dissecting cardosin B trafficking pathways in heterologous systems. *Planta* **2010**, *232*, 1517–1530. https://doi.org/10.1007/s00425-010-1276-9.
23. Simões, I.; Faro, C. Structure and function of plant aspartic proteinases. *Eur. J. Biochem.* **2004**, *271*, 2067–75. https://doi.org/10.1111/j.1432-1033.2004.04136.x.
24. Soares, A.; Ribeiro Carlton, S.M.; Simões, I. Atypical and nucellin-like aspartic proteases: Emerging players in plant developmental processes and stress responses. *J. Exp. Bot.* **2019**, *70*, 2059–2076. https://doi.org/10.1093/jxb/erz034.

25. Egas, C.; Lavoura, N.; Resende, R.; Brito, R.M.M.; Pires, E.; de Lima, M.C.P.; Faro, C. The Saposin-like Domain of the Plant Aspartic Proteinase Precursor Is a Potent Inducer of Vesicle Leakage. *J. Biol. Chem.* **2002**, *275*, 38190–38196. https://doi.org/10.1074/jbc.m006093200.
26. Terauchi, K.; Asakura, T.; Ueda, H.; Tamura, T.; Tamura, K.; Matsumoto, I.; Misaka, T.; Hara-Nishimura, I.; Abe, K. Plant-specific insertions in the soybean aspartic proteinases, soyAP1 and soyAP2, perform different functions of vacuolar targeting. *J. Plant Physiol.* **2006**, *163*, 856–62. https://doi.org/10.1016/j.jplph.2005.08.007.
27. De Moura, D.C.; Bryksa, B.C.; Yada, R.Y. In silico insights into protein-protein interactions and folding dynamics of the saposin-like domain of Solanum tuberosum aspartic protease. *PLoS ONE* **2014**, *9*, 18–22. https://doi.org/10.1371/journal.pone.0104315.
28. Frey, M.E.; D'Ippolito, S.; Pepe, A.; Daleo, G.R.; Guevara, M.G. Transgenic expression of plant-specific insert of potato aspartic proteases (StAP-PSI) confers enhanced resistance to Botrytis cinerea in Arabidopsis thaliana. *Phytochemistry* **2018**, *149*, 1–11. https://doi.org/10.1016/j.phytochem.2018.02.004.
29. Muñoz, F.; Palomares-Jerez, M.F.; Daleo, G.; Villalaín, J.; Guevara, M.G. Possible mechanism of structural transformations induced by StAsp-PSI in lipid membranes. *Biochim. Biophys. Acta Biomembr.* **2014**, *1838*, 339–347. https://doi.org/10.1016/j.bbamem.2013.08.004.
30. Törmäkangas, K.; Hadlington, J.L.; Pimpl, P.; Hillmer, S.; Brandizzi, F.; Teeri, T.H.; Denecke, J. A vacuolar sorting domain may also influence the way in which proteins leave the endoplasmic reticulum. *Plant Cell* **2001**, *13*, 2021–32.
31. De Caroli, M.; Lenucci, M.S.; Di Sansebastiano, G.-P.; Dalessandro, G.; De Lorenzo, G.; Piro, G. Protein trafficking to the cell wall occurs through mechanisms distinguishable from default sorting in tobacco. *Plant J.* **2011**, *65*, 295–308. https://doi.org/10.1111/j.1365-313X.2010.04421.x.
32. De Marchis, F.; Bellucci, M.; Pompa, A. Unconventional pathways of secretory plant proteins from the endoplasmic reticulum to the vacuole bypassing the Golgi complex. *Plant Signal. Behav.* **2013**, *8*. https://doi.org/10.4161/psb.25129.
33. Stigliano, E.; Faraco, M.; Neuhaus, J.-M.M.; Montefusco, A.; Dalessandro, G.; Piro, G.; Di Sansebastiano, G.-P. Pietro Two glycosylated vacuolar GFPs are new markers for ER-to-vacuole sorting. *Plant Physiol. Biochem.* **2013**, *73*, 337–343. https://doi.org/10.1016/j.plaphy.2013.10.010.
34. Sansebastiano, G.P. Di; Barozzi, F.; Piro, G.; Denecke, J.; Lousa, C.D.M. Trafficking routes to the plant vacuole: Connecting alternative and classical pathways. *J. Exp. Bot.* **2018**, *69*, 79–90. https://doi.org/10.1093/jxb/erx376.
35. Vieira, V.; Peixoto, B.; Costa, M.; Pereira, S.; Pissarra, J.; Pereira, C. N-linked glycosylation modulates Golgi-independent vacuolar sorting mediated by the plant specific insert. *Plants* **2019**, *8*, 312. https://doi.org/10.3390/plants8090312.
36. Matsushima, R.; Fukao, Y.; Nishimura, M.; Hara-Nishimura, I. NAI1 gene encodes a basic-helix-loop-helix-type putative transcription factor that regulates the formation of an endoplasmic reticulum-derived structure, the ER body. *Plant Cell* **2004**, *16*, 1536–1549. https://doi.org/10.1105/tpc.021154.
37. Bernat-Silvestre, C.; De Sousa Vieira, V.; Sánchez-Simarro, J.; Aniento, F.; Marcote, M.J. Transient Transformation of A. thaliana Seedlings by Vacuum Infiltration. *Methods Mol. Biol.* **2021**, *2200*, 147–155. https://doi.org/10.1007/978-1-0716-0880-7_6.
38. Nebenführ, A.; Ritzenthaler, C.; Robinson, D.G. Brefeldin A: Deciphering an enigmatic inhibitor of secretion. *Plant Physiol.* **2002**, *130*, 1102–1108. https://doi.org/10.1104/pp.011569.
39. Pereira, C.; Pereira, S.; Satiat-Jeunemaitre, B.; Pissarra, J. Cardosin A contains two vacuolar sorting signals using different vacuolar routes in tobacco epidermal cells. *Plant J.* **2013**, *76*, 87–100. https://doi.org/10.1111/tpj.12274.